



The rim zone of cement-based materials – Barrier or fast lane for chemical degradation?



M. Schwotzer^{a,*}, K. Konno^b, J. Kaltenbach^a, A. Gerdes^{a,c}

^a Karlsruhe Institute of Technology (KIT), Institute of Functional Interfaces, Hermann-von-Helmholtz-Platz 1, D-76344 Eggenstein-Leopoldshafen, Germany

^b Hokkaido University of Science, Department of Civil and Environmental Engineering, 4-1, 7-15, Maeda, Teine-ku, 006-8585 Sapporo, Japan

^c University of Applied Sciences Karlsruhe, Institute for Prevention in Construction, Moltkestr. 30, D-76133 Karlsruhe, Germany

ARTICLE INFO

Article history:

Received 4 June 2015

Received in revised form

9 October 2016

Accepted 13 October 2016

Available online 14 October 2016

Keywords:

Durability

Concrete

Surface layer

Transport properties

Cement paste

Microstructure

ABSTRACT

Sophisticated evaluation models for the long-term stability of cement-based systems demand a precise knowledge of the mechanisms of deterioration reactions, particularly respecting a permanent exposure to aqueous environments. Commonly, insights into these mechanisms are deduced from long-term investigations. However, these chemical reactions start immediately after exposure to aggressive environments causing rapid changes of composition and structure. Consequently, properties of its rim zone change, which affects transport processes in aqueous solutions. In laboratory experiments, the influence of these surface processes on the stability of cement-based materials exposed to different chloride solutions was studied as a function of time and temperature. Analysis of compositional and structural changes beneath the surface reveal the role of crystalline covering layers for chemical resistance. Such layers are often described as protective barriers. However, these processes in the rim zone can accelerate chemical degradation and subsequently reduce the resilience of the cement-based materials to aggressive aqueous environments.

© 2016 Elsevier Ltd. All rights reserved.

1. Introduction

Maximizing the service life of concrete structures as well as achieving an utmost long-term stability of cement bound waste forms, resulting from the solidification and stabilization of hazardous waste as potential final treatment prior to the disposal (e.g. Ref. [1]), are important challenges in the context of a sustainable development in construction and waste treatment. This holds true in particular for cement-based materials, which are permanently exposed to aggressive aqueous environments. With this in mind, rating material performance and precisely assessing the detrimental impact of aqueous environments is a major issue. In this regard, refined approaches in terms of an evaluation for the long-term behavior and durability are needed. A precondition for promising modeling approaches, in particular for service-life prediction, is a detailed and fundamental understanding of deterioration reactions. However, past research activities often showed no

clear and detailed picture of the reaction mechanism and the various factors determining the course of the damaging processes as denoted for sulfate attack [2] or in the context of the critical chloride content in steel reinforced concrete structures [3]. In order to characterize the material performance of cementitious systems, the behavior of these materials over time periods of weeks and months has mostly been studied [4]. Nevertheless, chemical reactions occur at the material/water interface and start immediately after exposure to aggressive environments. Transport processes are initiated due to concentration gradients between the alkaline pore solution of these highly porous materials and the surrounding aqueous media. Thus, chemical equilibrium between the pore solution and the solid phases will be disturbed and consequently dissolution and crystallization reactions are triggered. These reactive transport processes change the chemical and mineralogical composition of the material.

The first location where this reaction takes place is the near-surface region. This area also represents the first hurdle that must be overcome by an attacking aqueous solution. Thus, a crystalline covering layer on the surface of cement-based materials is said to act as a protective layer against reactive transport. This holds true in particular for carbonate precipitations on the surface of cement-

* Corresponding author.

E-mail addresses: matthias.schwotzer@kit.edu (M. Schwotzer), konno@hus.ac.jp (K. Konno), jonas.kaltenbach@kit.edu (J. Kaltenbach), andreas.gerdes@kit.edu (A. Gerdes).

based systems in contact with hard, carbonate-rich water, which hinders the transport and slows down e.g. the leaching process [5,6]. Also, the formation of $\text{Mg}(\text{OH})_2$ coatings as consequence of an attack by a MgSO_4 solution is assumed to restrict reactive transport processes [7].

However, the presence of carbonic acid species does not always lead to the formation of covering layers. In recent studies regarding the reliability of a specific leaching test for the evaluation of the stability of cement bound waste, the formation of a complex composed rim zone due to the presence of CO_2 was described. It was discussed whether this rim zone is potentially closely related to a non-satisfactory reproducibility of these tests [8–10]. It is announced that due to the development of complex chemical and mineralogical gradients, a modeling approach simply based on diffusion laws, in particular in an abundant presence of CO_2 , is not a promising way to extrapolate the long-term behavior based on the short-term experiment [9]. Similarly, the presumed protective effect of crystalline covering layers is closely related to the hydrochemistry of leachant and pore solutions, as well as to changes of the cement paste regarding permeability, cracking due to decalcification shrinkage [11], mineralogical and chemical composition [12]. In the case of calcium carbonate layers, it has been addressed that both the hydrochemical frame conditions during the growth of the covering layer and the mineralogical and structural evolution of the rim zone determine their effectiveness as a diffusion barrier [13]. Further, the reaction temperature is assumed to have an impact on the evolution of the properties of the rim zone due to reactive transport.

In order to illustrate the role of the rim zone for the chemical stability of cement paste samples, immersion experiments have been performed in salt solutions of different composition. This contribution focuses exemplarily on the chemical and mineralogical changes in the rim zone of cement paste samples exposed to different chloride solutions. A potential relation between temperature and the time dependant development of the material due to reactive transport processes will also be addressed.

2. Materials and methods

For the exposure tests with cement pastes, ordinary Portland cement (CEM I) was used to make prisms with a water to cement ratio of 0.5. For this, cement and water were mixed in a laboratory mixer and placed in $160 \times 40 \times 40$ mm molds and hydrated in the atmosphere of 20°C and 98% relative humidity for 24 h. The prisms were cured in tap water at 20°C for 32 days after demolding. The outer part of the prisms, where cement paste was in contact with water, was cut off and rectangular plates of $70 \times 30 \times 5$ mm were cut out. The plates were wrapped with polyvinylidene chloride foil to prevent shrinkage and kept for ten months at ~ 15 – 20°C .

0.8 mm thick slices were taken from the rectangular plates with a precision saw and stored under nitrogen atmosphere until the beginning of the experiment. Each sample was hung with a nylon string and placed into a plastic bottle filled with 70 mL of a solution. For the immersion test, four different chloride solutions were prepared: NaCl, KCl, MgCl_2 , and CaCl_2 , with a concentration of 1 mol/L of Cl^- , which is a common value for experimental work in the context of chloride attack on cement-based materials (e.g. Ref. [14]). Two additional experiments were carried out with hard tap water (saturation index for calcite of 0.32 (25°C) and for $\text{Ca}(\text{OH})_2$ of -10.7 (25°C), hardness of 2.66 mmol/L, calculated with PHREEQC [15]) and demineralized water, respectively. The immersion tests were carried out at a constant temperature of 20°C or 5°C in a closed system to inhibit a potential uptake of CO_2 .

The determination of the $\text{Ca}(\text{OH})_2$ and $\text{Mg}(\text{OH})_2$ content of the solid phases was performed with thermogravimetric analysis of

pulverized samples (TGA/SDTA 851, Mettler-Toledo). For electron microscopic investigations, an ESEM XL 30 FEG (Philips) equipped with an energy-dispersive X-ray spectroscopy system (EDX) (EDAX) was used. Surface sensitive X-ray diffraction (XRD) measurements were carried out with cement paste slices (D8 advance with $\text{Cu}_{\text{K}\alpha}$ radiation, Bruker). The composition of the reaction solutions was analyzed with Inductively Coupled Plasma- Atomic Emission Spectroscopy (ICP-AES) (Optima 8300, Perkin Elmer). The water soluble Cl^- content was determined by an aqueous extraction (1 g of a pulverized cement paste sample in 50 mL demineralized water) followed by a quantification of the anion content with ion chromatography (761 Compact IC, Metrohm).

3. Results

Fig. 1 shows the time dependant evolution of the composition of the solid phases regarding the $\text{Ca}(\text{OH})_2$ content (Fig. 1a) and the water soluble chloride content (Fig. 1d), as well as the leached quantity of Ca^{2+} (Fig. 1b) in the reaction solutions and their pH value (Fig. 1c), respectively.

The exposure to hard tap water did not lead to a significant leaching of the $\text{Ca}(\text{OH})_2$ and only a slight decrease of the Ca^{2+} concentration and the pH value was noted. The $\text{Ca}(\text{OH})_2$ content decreased significantly for all the other solutions. The loss of $\text{Ca}(\text{OH})_2$ in NaCl, KCl, and CaCl_2 solutions was more intense than in demineralized water and showed a similar behavior, whereas the most excessive loss of $\text{Ca}(\text{OH})_2$ was detected for the MgCl_2 solution (Fig. 1a). The reverse trend was observed for the calcium release (Fig. 1b). For most of the experiments, the pH values achieved a constant level of pH 11–12 during the first 24 h of the experiment. The immersion in the MgCl_2 solution did not lead to a high pH level and almost no change has been noticed in the pH value of the experiment performed with tap water (Fig. 1c). The uptake of Cl^- from the MgCl_2 and CaCl_2 solutions was more intense than from the NaCl and KCl solutions (Fig. 1d), generally resulting in the formation of Friedel's salt (identified in the bulk sample by means of XRD, not shown in this contribution).

Fig. 2 shows electron microscopic images of the cement paste surfaces after a 24 h exposure to different aqueous solutions. The pictures attached on the right hand side show the distribution of the element Ca analyzed in a cross section of the cement paste slices. Areas showing a significant decrease of Ca (attributed to a loss of $\text{Ca}(\text{OH})_2$) are surrounded with a white dotted line. A loss of $\text{Ca}(\text{OH})_2$ in the rim zones that have been in contact with the aqueous solutions was observed in the experiments with KCl, NaCl, CaCl_2 , and demineralized water (Fig. 2b, d-f).

After exposure to tap water, no significant leaching was noticed (Fig. 2a). The exposure to the MgCl_2 solution led to a complete loss of $\text{Ca}(\text{OH})_2$ (Fig. 2c). The microscopic view reveals a homogeneous deposition of crystalline reaction products only after the exposure to hard tap water and to the MgCl_2 solution.

In order to characterize potential crystalline reaction products on the surface of the cement paste samples, XRD investigations have been performed directly on the test specimen. The specimens have been mounted in the sample holders of the diffractometer without further preparation (such as grinding or drying). The results of the measurements after the immersion in the different aqueous solutions at 20°C for 24 h are shown in Fig. 3. The exposure to hard tap water led to a significant formation of calcite (Fig. 3a). The crystalline covering layer after exposure to the MgCl_2 solution was identified as $\text{Mg}(\text{OH})_2$ (brucite) (Fig. 3c). The investigation of the samples immersed in the NaCl, KCl, and CaCl_2 solutions showed only weak signals of calcite (Fig. 3d–f). After immersion in the KCl and CaCl_2 solutions, traces of Friedel's salt – and brucite in the case of CaCl_2 (Fig. 3f) potentially due to

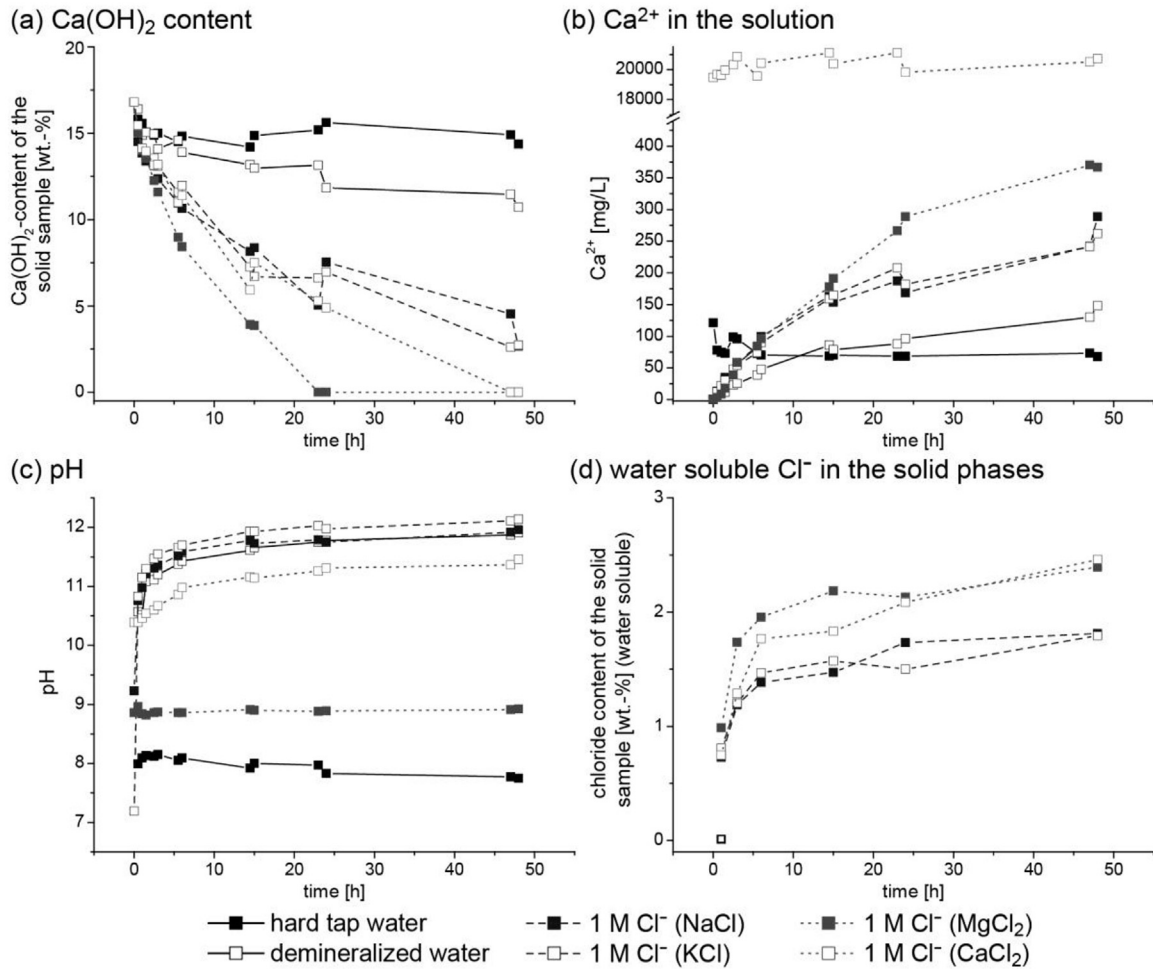


Fig. 1. Composition development of the solid phases and hydro chemical parameters of aqueous solutions as a function of time for the immersion tests with cement paste slices in different aqueous solutions at 20 °C: the Ca(OH)₂-content of the cement paste samples (a), the Ca²⁺ concentration (b) and the pH value (c) of the reaction solutions, and the water soluble chloride content of the cement paste samples (d).

impurities of Mg²⁺ in the salt solution, that have been proven by analysis of the aqueous solutions (not shown in this contribution, ICP-AES measurements) – appeared to be present in the area close to the surface of the samples (Fig. 3d and f). There was no experimental evidence for the occurrence of calcium or magnesium oxychloride phases in the surface near area of the samples after exposure to the Ca- and Mg-rich Cl⁻ solutions, although the formation of such phases seems to be likely under the present chemical boundary conditions [16]. The surface of sample exposed to demineralized water showed a significant signal of Ca(OH)₂ (portlandite) (Fig. 3b).

The electron microscopic images of a cement paste sample after 24 h exposure to a 1 M Cl⁻ solution based on MgCl₂ show an interweaved μ -crystalline covering layer of Mg(OH)₂. The structure of the covering layer formed at 20 °C is much finer (Fig. 4b) than the structure of the layer that was built up at 5 °C (Fig. 4a). At a reaction temperature of 20 °C, Ca(OH)₂ disappeared completely during exposure to the MgCl₂ solution, whereas at 5 °C a significant amount remained in the cement paste slice (Fig. 4c, Ca-results). At 20 °C, the Mg-rich reaction products are located mainly on the surface of the cement paste sample. In contrast to that, the sample from the 5 °C experiment shows the appearance of Mg-rich reaction products also in deeper areas beneath the surface. At both temperatures, chloride-rich areas appear to be located in distinct spots statistically spread over the whole area of the cross section.

Table 1 shows the results of the EDX analysis of the sample surface for the samples that have been exposed over 24 h to the 1 M Cl⁻ solution (MgCl₂) (shown in Fig. 4 a and b). The dense crystalline covering of the surface that has been immersed in the MgCl₂ solution at 20 °C appears to be mainly Mg(OH)₂. The results for the measurement on the surface of the sample at 5 °C show a significant content of the elements Si and Al. Furthermore, a higher amount of Ca was detected. However, these signals are supposed to originate from the cement paste substrate. The content of the element Cl is comparable for both exposure temperatures.

Fig. 5 shows the time dependent development of the depth resolved distribution of Ca in the cross sections of the cement paste slices. During the exposure to the MgCl₂ solution at 20 °C, a continuous depletion of Ca(OH)₂ was detected as indicated by the white dashed lines (Fig. 5a). Over time, the degradation of Ca(OH)₂ was affecting deeper areas of the material, whereas the newly built Mg(OH)₂ is mainly located on top of the surface of the samples (Fig. 5a). The results of the time resolved determination of the content of Ca(OH)₂ and Mg(OH)₂ in the cement paste samples are shown in Fig. 5b.

How fast such layers can develop as a consequence of the exposure to an aggressive aqueous environment is revealed by means of high resolution ESEM investigations (Fig. 6). The overview image of the sample that was subjected to hard tap water for 1 min did not show any noticeable features that indicate chemical

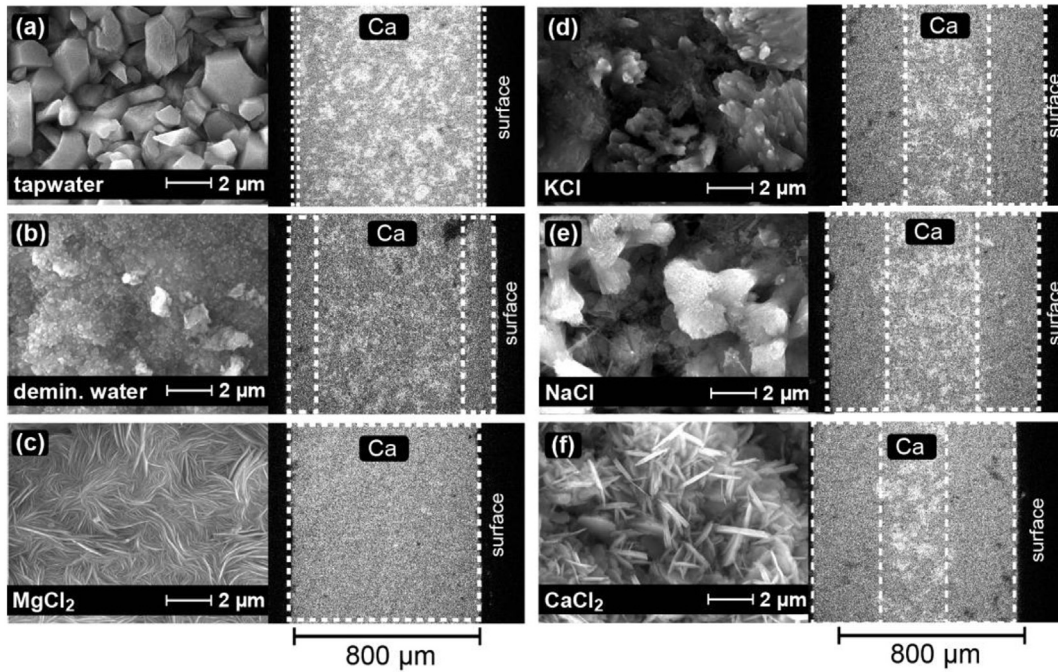


Fig. 2. Electron microscopic images of the surface of the cement paste samples and Ca-mappings on a fracture surface on the sample cross-sections after exposure to the different aqueous solutions such as hard tap water (a), demineralized water (b) as well as solutions of MgCl₂ (c), KCl (d), NaCl (e), and CaCl₂ (f) for 24 h at 20 °C. Areas with a significant content of Ca(OH)₂ show up as brighter spots in the Ca-mappings.

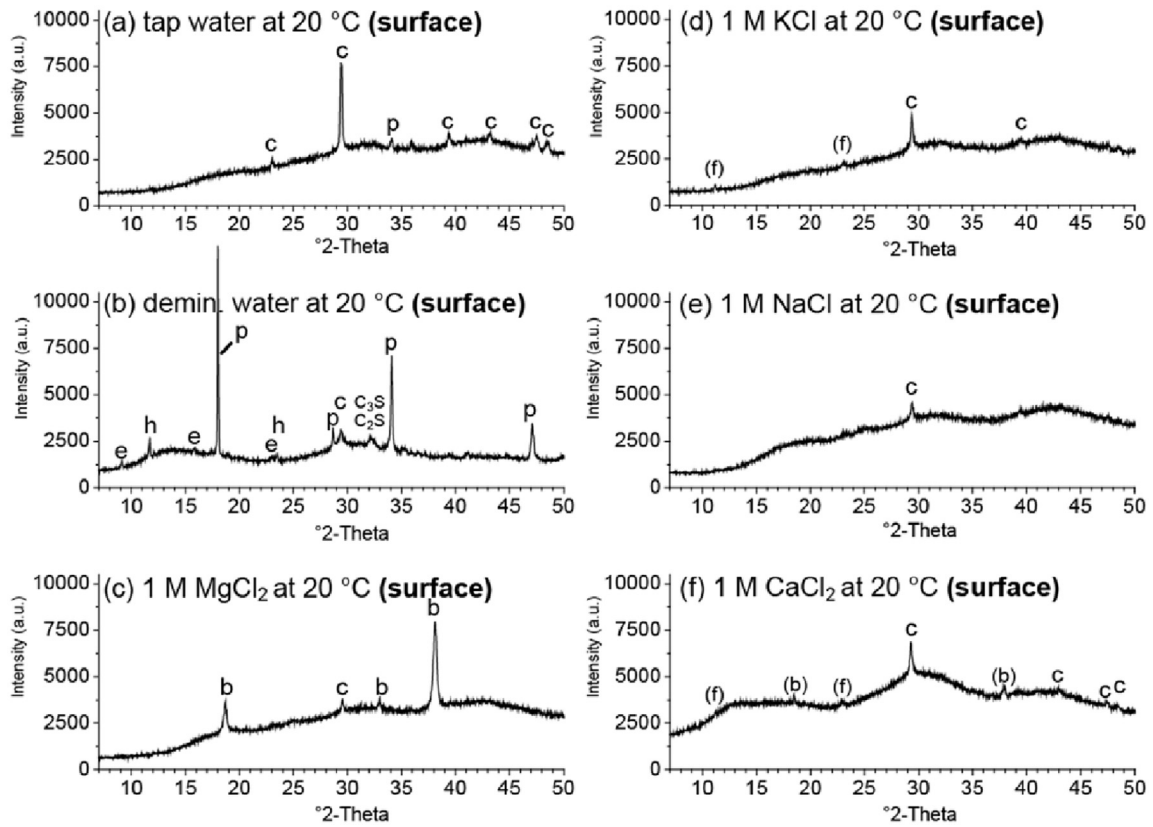


Fig. 3. Results of the XRD investigation of the surface of the cement paste slices after the immersion in different aqueous solutions as hard tap water (a) and demineralized water (b) as well as solutions of MgCl₂ (c), KCl (d), NaCl (e), and CaCl₂ (f) at 20 °C for 24 h. b: brucite, c: calcite, e: ettringite, h: hydroxalite, f: Friedel's salt, p: portlandite, and C₃S/C₂S; a.u.: arbitrary units.

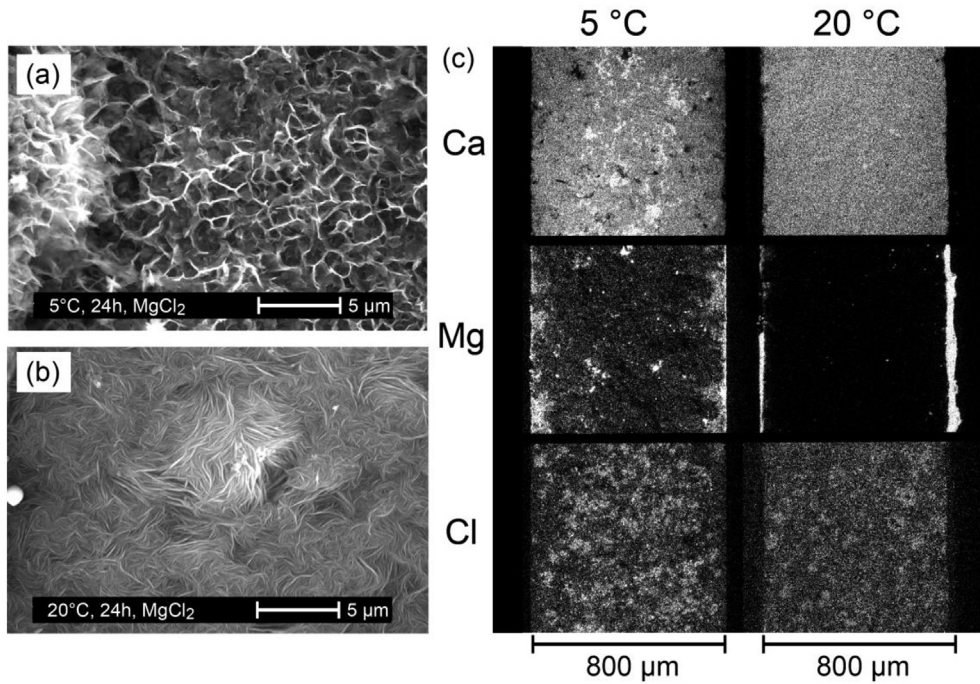


Fig. 4. Electron microscopic images of the surface of the cement paste samples after exposure to a 1 M Cl^- solution (MgCl_2) kept for 24 h at 5 °C (a) and 20 °C (b). Element mappings for the elements Ca, Mg, and Cl measured on cross sections are shown for both, 5 °C and 20 °C; areas with a high content of the respective element show up as brighter spots in the mappings compared to areas with a lower content (c).

Table 1
Results of the integral EDX investigations performed on the surfaces of cement paste samples after exposure to a 1 M Cl^- solution (MgCl_2) kept for 24 h at 5 °C and 20 °C (shown in Fig. 4a and b).

Experiment	O [At.-%]	Na [At.-%]	Mg [At.-%]	Al [At.-%]	Si [At.-%]	S [At.-%]	Cl [At.-%]	K [At.-%]	Ca [At.-%]
24 h at 5 °C	71.0	0.5	12.9	1.0	4.2	0.1	0.5	0.2	9.4
24 h at 20 °C	68.9	n.d.	27.7	n.d.	0.1	n.d.	0.4	n.d.	3.0

n.d.: not detected; At.-%: atom percent.

changes on the sample surface (Fig. 6a, upper image). No significant differences to a fresh cut sample surface without exposure to an aqueous solution were observed (not shown). Only an examination under higher magnification revealed a beginning growth of

carbonate minerals (Fig. 6a, lower image). In contrast to that, the surface of the sample that has been exposed for the time period of 1 min to a 1 M Cl^- solution (MgCl_2) showed a conspicuous pattern of micro cracks (Fig. 6b, upper image). The surface was covered

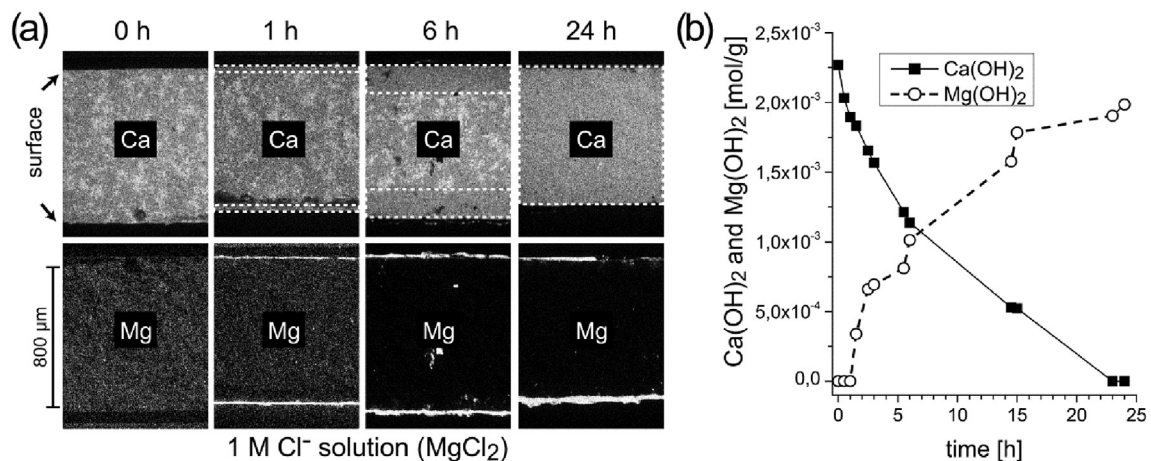


Fig. 5. Element mappings for the elements Ca and Mg on cross sections of cement paste samples immersed for 0, 1, 6, and 24 h in a 1 M Cl^- solution (MgCl_2) kept at 20 °C. The $\text{Ca}(\text{OH})_2$ -depleted areas are indicated by dashed lines (a). Content of $\text{Ca}(\text{OH})_2$ and $\text{Mg}(\text{OH})_2$ in the cement paste samples as a function of time [mol/g] (b).

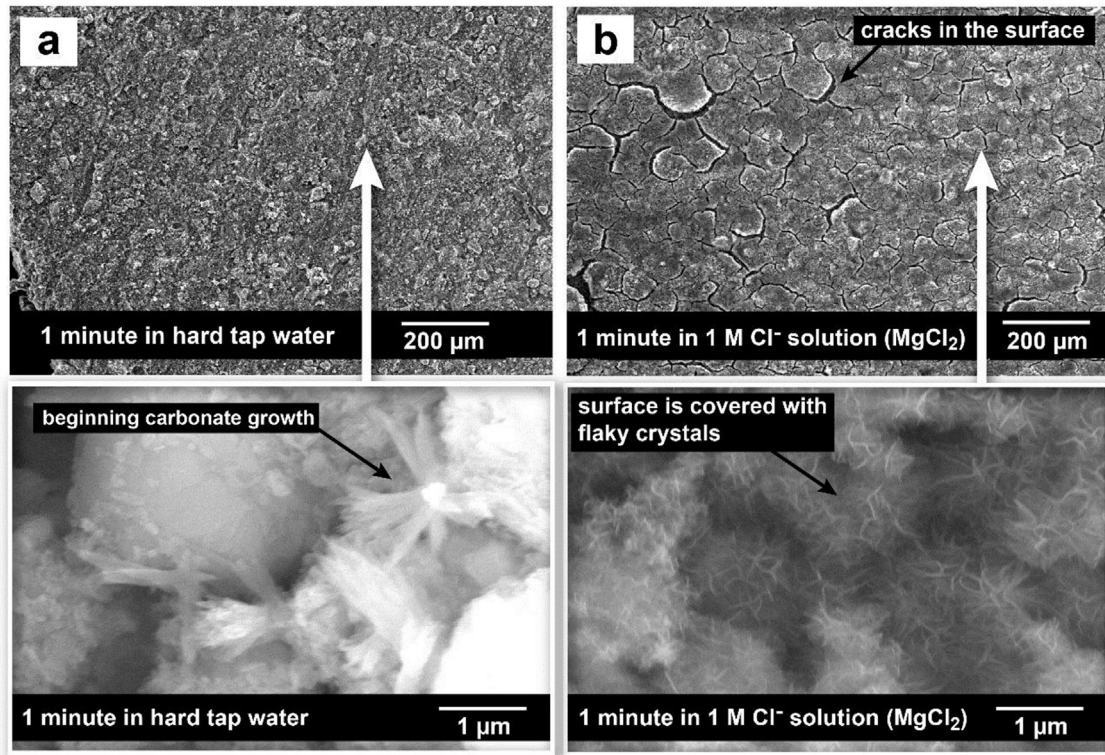


Fig. 6. Electron microscopic images of the surface of the cement paste samples after 1 min exposure to hard tap water (a) and a 1 M Cl⁻ solution (MgCl₂) (b). The upper images show an overview and the lower images show the sample surface at higher magnification (20 °C).

completely with nanoscale flaky crystals (Fig. 6b, lower image).

Fig. 7 shows the results of electron microscopic investigations on cross sections of a cement paste sample that has been immersed in a 1 M Cl⁻ solution based on MgCl₂ for 5 days at 20 °C. The structure of the Mg(OH)₂ layer appears compact and dense.

4. Discussion

Regarding the results of the laboratory experiments, two experiments were particularly distinct. The experiments with tap water showed that the contact between the cement paste samples and hard tap water did not lead to significant changes in the

composition of the solid samples or of the reaction solution (Fig. 1b and c). This can be attributed to the formation of a calcium carbonate layer on the surface of the cement paste (Fig. 3a), which may act as a diffusion barrier and thus, provide a protection against reactive transport processes. The slight decrease of the Ca²⁺ content in the solution over time (Fig. 1b) indicates that the growth of this layer occurs within the first few hours. It is reported that CaCO₃ layers, which grow on the surfaces of cement-based systems as a consequence of a contact with hard tap water, develop a dense structure providing a protection against reactive transport processes [17].

As well, the exposure to the MgCl₂ solution leads to the formation of a dense appearing layer of crystalline reaction products (Fig. 7) capping completely the sample surface (Fig. 2c). In contrast to the tap water exposure, the results of the experiments with the MgCl₂ solutions show features of an intense attack despite the presence of the crystalline covering layer. In the exposure experiment with the MgCl₂ solution, the degradation rate of Ca(OH)₂, as well as the Ca²⁺ release, was higher than in all other experiments (Fig. 1). Additionally, the formation of a Mg(OH)₂ covering layer (Figs. 5 and 6) did not inhibit the chloride ingress compared to the other experiments with chloride solutions (Fig. 1d). Only the pH value of the reaction solution remained stable and relatively low. But this is no sign of “dormancy” in the attack by reactive transport processes. It rather indicates a crystallization process. The transport of OH⁻ into the reaction solution, responsible for the rising pH value in all the other experiments (Fig. 1), feeds an intensive crystallization of Mg(OH)₂ on the sample surface. This process is consuming OH⁻ and, therefore, continuously triggering a permanent dissolution of Ca(OH)₂. This causes intense changes of the mineralogical composition and affects, consequently, the structural properties, such as an increasing porosity [18]. Similar results have also been reported for an exposure to MgSO₄ solutions [19].

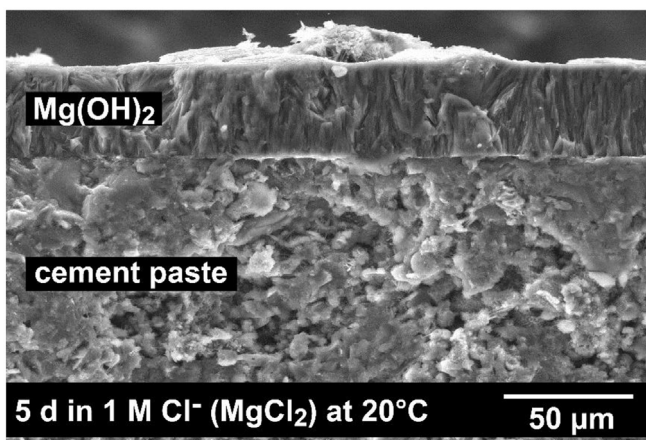


Fig. 7. Electron microscopic image of a cross section of a cement paste sample immersed for 5 d in a 1 M Cl⁻ solution (MgCl₂) at 20 °C.

Nevertheless, it is still often supposed that covering layers of $\text{Mg}(\text{OH})_2$ provide a barrier against reactive transport processes, as stated in particular for a MgSO_4 environment [7,20,21].

These two extreme results, on the one hand for calcium carbonate covering layers grown on cement-based materials in contact with hard tap water, and on the other hand thick covering layers by $\text{Mg}(\text{OH})_2$ due to exposure to the MgCl_2 solution, show that an evaluation of protective or non-protective properties of crystalline covering layers has to be based on differentiated examinations focusing on the evolution of the properties of the rim zone of the material.

Compared to the growth of CaCO_3 on the surfaces of cement paste samples after exposure to hard tap water, the formation of $\text{Mg}(\text{OH})_2$ due to the exposure to a MgCl_2 -solution occurs significantly faster (Fig. 6). Moreover it is remarkable, that the growth of $\text{Mg}(\text{OH})_2$ is accompanied by an extensive formation of microcracks on the surface. The crystallization of $\text{Mg}(\text{OH})_2$ on the surface is fed by the dissolution of $\text{Ca}(\text{OH})_2$ (Fig. 5b). Furthermore, the calcium silicate hydrate phases (CSH) may be subjected to a chemical attack potentially resulting in the formation of magnesium silicate hydrate phases (MSH) - as often reported in this context [7,22]. Such a chemical degradation of these main compounds of hardened cement paste is supposed to be closely related to the formation of microcracks [11,23]. The short-term exposure experiments show that a contact to the MgCl_2 solution immediately affects the composition and structure of the several μm thick rim zone of the material. Even though this process is followed by a quick formation of a thick layer of flaky $\text{Mg}(\text{OH})_2$ crystals (Figs. 3c and 5a), it appears to be obvious that the consequence of this micro structural evolution cannot be an increased protection against reactive transport processes.

In the other experiments performed with demineralized water, alkali chloride solutions and the CaCl_2 solution, no significant formation of potentially protective covering layers and no development of transport inhibiting properties in the rim zone were observed (Fig. 2 d–f and Fig. 3 d–f). Regarding the reaction velocity, these solutions take an intermediate position between the slowest (tap water) and the fastest (MgCl_2).

Nevertheless, in all cases, the degradation of $\text{Ca}(\text{OH})_2$ in the cement paste, coupled with a Ca^{2+} release into the reaction solution, affects the exposed material to more than a 500 μm depth within 24 h (Fig. 2). This also holds true for the uptake of chlorides in the cement paste occurring mainly within the first 6 h of the experiment (Fig. 1d). However, the structural properties of the sample surface differ significantly depending on the composition of the surrounding aqueous solutions (Fig. 2). In addition, the temperature during the experiments has a strong impact on the evolution of the properties on the surface, as well as within the rim zone of a cement-based system. In the case of MgCl_2 exposure, the structure of the $\text{Mg}(\text{OH})_2$ layers is closely related to the temperature (Fig. 4a and b) affecting, in turn, the reactive transport processes. In this regard, the occurrence of other Mg-rich phases, such as Mg-oxychloride phases - especially at low temperatures - as described in the literature [14,16], should be mentioned. However, in this study no experimental evidence for this was noticed, neither by means of XRD (Fig. 3) nor by EDX investigations (Table 1).

The proceeding of the discharge of $\text{Ca}(\text{OH})_2$ at 5 °C is much slower than at 20 °C. In addition, a significant formation of Mg-compounds below the surface on the way to the interior of the material was observed (Fig. 4c). However, this might be also attributed to the temperature dependence of the solubility of relevant compounds, e.g. the increasing solubility of $\text{Mg}(\text{OH})_2$ with decreasing temperature [24]. In this way, the chemical reactions affect the transport processes and vice versa and both are associated with the temperature. Temperature has a significant effect on

the equilibria between solid phases and pore solution in relevant systems [25] and, furthermore, on the solubility of gases in aqueous solutions. The latter is of particular importance when carbonic acid species are involved in the reactions.

The rim zone of cement-based materials in contact with every kind of aqueous solution acts as a “chemical/mineralogical process zone” determining the transport properties and affecting, in turn, the durability of the materials. In this context, the development of crystalline covering layers plays a key role. These layers may act as a diffusion barrier when their growth does not harm the underlying structure and composition of the cement paste substrate as in the cases of CaCO_3 due to the exposure to hard water, because Ca^{2+} and CO_3^{2-} are provided commonly from the hard water [17]. The deposition of the products of a degradation reaction, for instance as $\text{Mg}(\text{OH})_2$ as a consequence of an attack by a Mg^{2+} rich solution consuming OH^- from the $\text{Ca}(\text{OH})_2$ compound of the cement paste, is not supposed to provide a protective effect. Moreover, this process triggers a further degradation.

5. Concluding remarks

These results highlight the complexity of physico-chemical processes affecting the properties of a several μm thick rim zone of Portland cement bound systems and, therefore, determining, if it acts as protective barrier or fast lane for reactive transport processes. Its structural properties, especially the capacity to inhibit transport processes, which protects the cement paste, are closely related to the boundary conditions during crystal growth. In the case of calcium carbonate on the surface of cement paste exposed to hard tap water, the structure of the covering layers is often dense and able to restrict transport processes. In contrast, the formation of the $\text{Mg}(\text{OH})_2$ capping due to the impact of the MgCl_2 solution occurs in a way that harms the cement paste substrate and does not provide a protective effect. Hence, such a chemical attack instantly causes the alteration of a several tens of μm thin rim zone of a cement-based material.

The development of the chemical and structural properties of the rim zone is closely related to the evolution of chemical degradation by means of reactive transport. Accordingly, processes that occur on the material surfaces within a very short time period may seriously affect the resistance against chemical attacks of a cement-based material and, thus, its durability. The relevance of such surface processes for the resistance against reactive transport processes emphasizes in particular the importance of the curing phase for the vulnerability of cementitious systems to chemical degradation.

Acknowledgments

We are grateful to Marita Heinle for the ICP-AES measurements. Olivia Wenzel, Dr. Dominik Dannheim, and Tim März are greatly acknowledged for their substantial support.

References

- [1] F.P. Glasser, *Fundamental aspects of cement solidification and stabilisation*, J. Hazard. Mater 52 (1997) 151–170.
- [2] A. Neville, *The confused world of sulfate attack on concrete*, Cem. Concr. Res. 34 (2004) 1275–1296.
- [3] U. Angst, B. Elsener, C.K. Larsen, Ø. Vennesland, *Critical chloride content in reinforced concrete — A review*, Cem. Concr. Res. 39 (2009) 1122–1138.
- [4] Y. Maltais, E. Samson, J. Marchand, *Predicting the durability of Portland cement systems in aggressive environments—Laboratory validation*, Cem. Concr. Res. 34 (2004) 1579–1589.
- [5] E. Koelliker, *Calciumcarbonate and their significance for the corrosion of concrete*, in: Proc. 8th Int. Congr. Chem. Cem., Rio de Janeiro, 1986.
- [6] M. Moranville, S. Kamali, E. Guillon, *Physicochemical equilibria of cement-based materials in aggressive environments—experiment and modeling*,

- Cem. Concr. Res. 34 (2004) 1569–1578.
- [7] M. Santhanam, M.D. Cohen, J. Olek, Mechanism of sulfate attack: a fresh look: Part 2. Proposed mechanisms, *Cem. Concr. Res.* 33 (2003) 341–346.
- [8] M. Andac, F.P. Glasser, The effect of test conditions on the leaching of stabilised MSWI-fly ash in Portland cement, *Waste Manag.* 18 (1998) 309–319.
- [9] M. Andac, F.P. Glasser, Long-term leaching mechanisms of Portland cement-stabilized municipal solid waste fly ash in carbonated water, *Cem. Concr. Res.* 29 (1999) 179–186.
- [10] T. Van Gerven, J. Moors, V. Dutré, C. Vandecasteele, Effect of CO₂ on leaching from a cement-stabilized MSWI fly ash, *Cem. Concr. Res.* 34 (2004) 1103–1109.
- [11] J.J. Chen, J.J. Thomas, H.M. Jennings, Decalcification shrinkage of cement paste, *Cem. Concr. Res.* 36 (2006) 801–809.
- [12] M. Schwotzer, A. Gerdes, Durability of cement based materials in contact with drinking water, in: *Concrete in Aggressive Aqueous Environments - Performance, Testing, and Modeling*, RILEM Proceedings PRO 60, Toulouse, France, 2009, pp. 125–132.
- [13] M. Schwotzer, Zur Wechselwirkung zementgebundener Werkstoffe mit Wässern unterschiedlicher Zusammensetzung am Beispiel von Trinkwasserbehälterbeschichtungen, Universität Karlsruhe (TH), Germany, 2008. PhD thesis.
- [14] K. Peterson, G. Julio-Betancourt, L. Sutter, R.D. Hooton, D. Johnston, Observations of chloride ingress and calcium oxychloride formation in laboratory concrete and mortar at 5 °C, *Cem. Concr. Res.* 45 (2013) 79–90.
- [15] D.L. Parkhurst, User's guide to PHREEQC — a computer program for speciation, reaction-path, advective transport, and inverse geochemical calculations, in: *Water-Resources Investigations Report 95-4227*, United States Geological Survey, Lakewood, CO, 1995.
- [16] L. Sutter, K. Peterson, S. Touton, T. Van Dam, D. Johnston, Petrographic evidence of calcium oxychloride formation in mortars exposed to magnesium chloride solution, *Cem. Concr. Res.* 36 (2006) 1533–1541.
- [17] M. Schwotzer, T. Scherer, A. Gerdes, Protective or damage promoting effect of calcium carbonate layers on the surface of cement based materials in aqueous environments, *Cem. Concr. Res.* 40 (2010) 1410–1418.
- [18] K. Haga, M. Shibata, M. Hironaga, S. Tanaka, S. Nagasaki, Change in pore structure and composition of hardened cement paste during the process of dissolution, *Cem. Concr. Res.* 35 (2005) 943–950.
- [19] M. Schwotzer, T. Scherer, A. Gerdes, Immediate impact on the rim zone of cement based materials due to chemical attack: a focused ion beam study, *Mater. Charact.* 99 (2015) 77–83.
- [20] M. Santhanam, M. Cohen, J. Olek, Differentiating seawater and groundwater sulfate attack in Portland cement mortars, *Cem. Concr. Res.* 36 (2006) 2132–2137.
- [21] M. Santhanam, Test methods for magnesium attack, in: M. Alexander, A. Bertron, N. De Belie (Eds.), *Performance of cement-based materials in aggressive aqueous environments: state-of-the-art report*, RILEM TC 211 – PAE, Springer Netherlands, Dordrecht, 2013, pp. 345–354.
- [22] D.R.M. Brew, F.P. Glasser, Synthesis and characterisation of magnesium silicate hydrate gels, *Cem. Concr. Res.* 35 (2005) 85–98.
- [23] T. Rougelot, N. Burlion, D. Bernard, F. Skoczylas, About microcracking due to leaching in cementitious composites: X-ray microtomography description and numerical approach, *Cem. Concr. Res.* 40 (2010) 271–283.
- [24] M. Hänchen, V. Prigiobbe, R. Baciocchi, M. Mazzotti, Precipitation in the Mg-carbonate system—effects of temperature and CO₂ pressure, *Chem. Eng. Sci.* 63 (2008) 1012–1028.
- [25] M. Balonis, B. Lothenbach, G. Le Saout, F.P. Glasser, Impact of chloride on the mineralogy of hydrated Portland cement systems, *Cem. Concr. Res.* 40 (2010) 1009–1022.